Comparison of Exploration Portable Life Support Subsystem (xPLSS) Thermal Modeling to Thermal Vacuum Testing

Chane Sladek[1] and Noah Andersen[2]
HX5, LLC (NASA JSC)

Emma Goodman[3] and Michael Lewandowski[4]
Jacobs Engineering (NASA JSC)

and

David Westheimer[5]
NASA JSC

To support NASA's goal to return to the Moon through the Artemis mission, the development of an exploration portable life support system (xPLSS) has been conducted at Johnson Space Center (JSC). As part of this development process, a large system level thermal/fluid model of the xPLSS was developed using Thermal Desktop and an in-house human model (METMAN). The xPLSS model was used throughout the design process to predict the performance and temperature of nearly all components within the xPLSS.

In the fall of 2023, the design, verification, and testing (DVT) unit of the xPLSS was tested in a thermal vacuum (TVAC) chamber at JSC. This testing consisted of combining the xPLSS with an upper torso of the exploration pressure garment system (xPGS) and simulating five extravehicular activities (EVAs) in extreme thermal conditions (two cold EVAs and three hot EVAs). The data generated in this test series provided system level data of the xPLSS operating in vacuum and at flight-like environmental temperatures for the first time. This data was compared to results output by the xPLSS system model to assess the accuracy of previous analyses and improve the fidelity and accuracy of the xPLSS system model. The comparison between model and test hardware provides valuable insight that will help improve the design and fidelity of next generation space suits. In general, comparison between test data and model data generally showed slightly un-conservative values (model predicting colder temperatures than test in hot environments, and hotter temperatures than test in cold environments). Model assumptions and test assumptions were assessed to understand potential causes of some of these sources in error. Recommendations to improve the fidelity of the xPLSS model were also made based on the results presented in this paper.

[1] Thermal Analysis Engineer, JETS II, NASA JSC
[2] Thermal Analysis Engineer, JETS II, NASA JSC
[3] Chemical Engineer – Modeling & Simulation, JETS II, NASA JSC
[4] Thermal Analysis Engineer, JETS II, NASA JSC
[5] PLSS Development Engineer, NASA JSC

Nomenclature

ATCL	=	auxiliary thermal control loop
CO_2	=	carbon dioxide
CWS	=	caution and warning system
DVT	=	design, verification, and testing
EPG	=	environmental protection garment
EVAs	=	extravehicular activities
HMS	=	human metabolic simulator
HUT	=	hard upper torso
ISS	=	International Space Station
JSC	=	Johnson Space Center
LCVG	=	liquid cooling and ventilation garment
MiniME	=	mini membrane evaporator
POA	=	primary oxygen assembly
PTCL	=	primary thermal control loop
RCA	=	rapid cycle amine
SOA	=	secondary oxygen assembly
SWME	=	spacesuit water membrane evaporator
SxEMU	=	short extravehicular mobility unit
TD	=	Thermal Desktop
TC	=	thermocouple
TVAC	=	thermal vacuum
xINFO	=	exploration information system
xPGS	=	exploration pressure garment system
xPLSS	=	exploration portable life support subsystem

I. Motivation

WITH the goal of returning astronauts to the Moon for the first time in over 50 years, and the development of the lunar space station, Gateway, the time has come for the development of a new extravehicular mobility unit (EMU), or spacesuit. This innovation, called the exploration extravehicular mobility unit (xEMU), comprises the exploration portable life support system (xPLSS) and the exploration pressure garment system (xPGS). This paper covers the thermal model validation regarding the xPLSS. The goal of any model is to be able to simulate scenarios for both the system in question and its surroundings to learn how the system will behave or interact with its surroundings. The thermal xPLSS model is used to study the movement of heat throughout the system when the system is running nominally. The way the system operates must be understood thoroughly and modeled to reflect what might happen in real scenarios. A robust model can allow its user to study numerous cases without having to expend physical resources and hardware; rely on availability, willingness, and capability of staff to support experiments; and take up long periods of time to study just one case. Because models can be used so easily to simulate a variety of scenarios, they must be accurate. Model development and system design go hand-in-hand as iterative processes that require tuning, tweaking, and validation. The xPLSS model was compared to thermal vacuum (TVAC) test results, and data from each were used to enhance the other. Some aspects of the xPLSS model were validated by studying TVAC test results, and some parts of the model were tuned to be more accurate using the results from actual test data. Models are never going to be perfect, but tuning them and verifying them using actual experimental results is essential for any model output to be trustworthy or applicable, to the point where its output can inform design decisions with reasonable confidence. TVAC testing specifically provides data in vacuum environments at extreme temperatures, the surroundings in which xEMUs are expected to operate. By gathering data from tests such as this, the xPLSS model can be enhanced and verified using conditions that are more representative of what will be experienced by users of the xEMU. Experiments like these are critical for developing an accurate and useful model.

II. Background

A. Background of xPLSS Model

The xPLSS model was developed to provide accurate system-level thermal and fluid analyses to help guide the design and development of the xPLSS[1]. The model was generated by integrating the 41 node Metabolic Man simulation model (METMAN) with a Thermal Desktop® (TD) model of all components within the xPLSS. METMAN is used to represent the human in the system by providing fluid flow inputs to the xPLSS model (e.g. ventilation loop temperature, carbon dioxide (CO_2) production, crewmember latent load) based on the workload of the crewmember and environment conditions. The model correlation effort documented in this paper will be primarily focused on the xPLSS side of the model, as there was no human in the loop for this test series. The xPLSS model can be broken into two distinct modules – the thermal model and the fluid module.

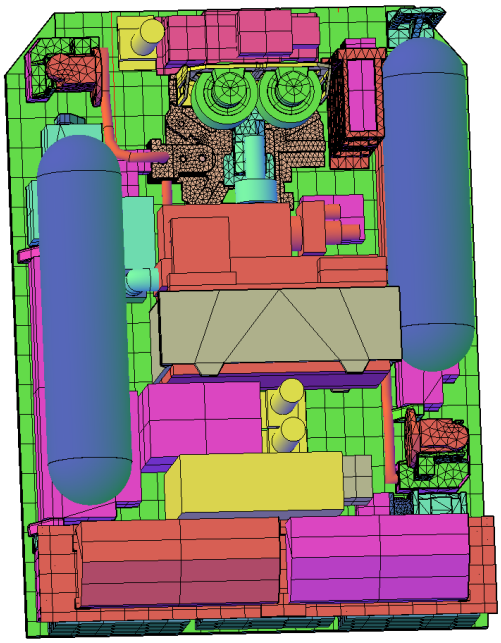

Figure 1. Geometry of the xPLSS model.

The thermal module consists of the physical structures within the PLSS (See Figure 1). The thermal model contains the three main types of heat transfer present within the xPLSS. Radiation heat transfer between various subsystems within the xPLSS is accounted for using the RADCAD capabilities of TD. Where possible, primitive geometries such as rectangles, cylinders and boxes, are used to accurately represent conduction within components. When higher fidelity geometry was needed, SpaceClaim was used to generate non structured thermal meshes. Conduction between components is modeled using test data (when available), empirical relationships (when applicable), and conservative assumptions based on engineering judgement. Convection from the gases with the ventilation and transport loop is modeled through empirical relationships and coupling the fluid module of the model with the thermal module of the model. Heat dissipation from the operation of control boxes, fans, pumps, valves, and other components is input into the model by applying heat loads onto the nodes at appropriate locations within the xPLSS model.

The fluid module uses FloCAD to model the oxygen ventilation loop (OVL), primary and secondary oxygen loops, primary thermal control loop (TCL) and auxiliary thermal control loop (ATCL). This allows for modeling of the flow of heat from the fluid loops to the xPLSS, species tracking within the various subsystems (such as removal of CO_2 from the ventilation loop) and various operational modes implemented while operating the PLSS (i.e. adjustments of the thermal control valve by the crewmember). The fluid module interacts with the thermal module primarily through the flow of heat from the fluids to the components; however, it also interacts through impacts on the performance. As an example, the CO_2 generation within the loop may influence how often the rapid cycle amine (RCA) needs to adjust the flow field through the two adsorbing/desorbing beds, which impacts the total heat dissipation coming off of the CO_2 removal technology via the RCA.

The TD xPLSS model has historically been used for a wide variety of analyses. One common use case of the xPLSS model is to use the model to generate accurate boundary conditions for a higher-fidelity, detailed model. Generating a very high-fidelity model of every component in the xPLSS would result in a model that was slow to run and could not produce analysis results in a reasonable time frame. For this reason, this model could be run first to provide the high-fidelity model with a more accurate boundary condition. This approach was used to investigate electronic boxes,[2,3,4,5,6] various potentiometers and actuators throughout the xPLSS,[7,8] CO_2 sensors,[9] battery assemblies,[10] and antennas.[11] Another use of the model was to simulate extravehicular activities (EVAs) to predict the performance of both the complete xPLSS and individual components under both nominal[12,13] and emergency procedures.[14,15] The model was also used to generate algorithms to automatically control crewmember cooling.[16]

Before completion of fully integrated thermal vacuum testing of the xPLSS in realistic conditions, there was system level dataset that could be used to correlate the xPLSS model. In lieu of full system test data, the analysts relied on component level testing, empirical relationships, and conservative assumptions to ensure the accuracy of analyses. These provide useful data that increase the confidence of the model but cannot perfectly represent the complete system

when operating in a realistic environment with a fully integrated xPLSS. Comparing the xPLSS model to the results from the thermal vacuum Chamber B test series will further improve the fidelity and accuracy of the system model by helping to close these gaps and uncertainties.

B. Background of TVAC Test

The thermal vacuum tests in Chamber B at Johnson Space Center are the highest fidelity and most flight-like test of the xEMU to date. Two test articles were present for Chamber B testing, a full xPGS without the xPLSS known as Suit 2, and a short xEMU (SxEMU) consisting of the xPLSS, the aluminum Hard Upper Torso (HUT), a helmet assembly, the Exploration Information System (xINFO) lighting band and camera, and a Human Metabolic Simulator (HMS) to introduce simulated human metabolic products. The HMS, originally intended to inject metabolic CO_2 and moisture, had to be downscoped to not inject moisture during the test due to substantial risk of condensation. For this reason, the metabolic impacts of a human in the loop were only partially realized during the test series (CO_2 injection and sensible heat). During this test series, five 8-hour EVAs were simulated over the course of 116 total test hours by collecting data over the widest possible temperature range at vacuum conditions. This temperature range was selected to encompass the range of temperatures experienced during EVAs on the International Space Station (ISS) as well as the lunar surface. Overall, the test served three main purposes: running the xEMU in vacuum conditions allowing for sub-ambient operation of the suit and its internal hardware, simulating operation in space-like conditions (vacuum and cold/hot temperatures), and testing a fully integrated spacesuit assembly. Both suits (SxEMU and Suit 2) were covered in over 100 thermocouples to identify the temperatures of the suits at important locations. xPLSS data gathered from the SxEMU test article results fed into the validation and updating of the xPLSS thermal model; this consisted of information regarding the performance of the internal hardware of the xPLSS, xPGS hatch, and xPGS HUT during the simulated EVAs. A more thorough overview of the xEMU TVAC testing is provided in the Thermal Vacuum Test Overview[17].

III. Approach

The goal of this study, as has been stated, was to assess the fidelity of the xPLSS simulation model in TD through comparisons to SxEMU TVAC test data. The original xPLSS model, however, was built based on the full xEMU with metabolic loads from an actual crewmember (modeled using METMAN). Although the SxEMU *partially* represents the full xEMU and the inputs of the HMS *partially* represent the inputs of a real crewmember, the differences between each of them and the assumptions of the xPLSS model are large enough to impact results. Therefore, the modeling approach in the current study was primarily concerned with making the necessary adjustments to minimize those differences. These included decoupling major logic controls and replacing them with user-defined, constant inputs, adjusting power dissipation levels in electronic components, flipping control switches, and tuning the environment temperature.

Within the xPLSS model, there are logic controls written in Fortran that integrate the behavior of many components with METMAN, which is run in tandem with the model. Rather than changing METMAN to function like the HMS instead of a theoretical crewmember, the logic controls were changed to ignore the crucial variables passed from METMAN and those variables were set to user-defined, constant parameters. This included the metabolic fluid inputs, exhaled CO_2 and H_2O vapor, as well as crew heat exchange to the Liquid Cooling and Ventilation Garment (LCVG). These values are case dependent; however, due to the limitations of the HMS, H_2O vapor input is zero in all cases. Further, there are logic controls dictating the Thermal Control Valve (TCV) position based on the heat storage of the METMAN crewmember. This connection was also severed and the TCV set to a "full-open" state where 100% of the primary loop water flow goes through the LCVG and none through the bypass. This was the configuration used during all EVAs in TVAC testing.

Beyond logic controls, there were several user-defined parameters that had to be changed to match the actual test setup. The fluid loops require flow rates, which were measured during the test. The model also requires a suit free volume, which was estimated based on pressure decay rates during airlock depress. Further, power dissipation values can be added to all major electrical components. The motors, pumps, and fans were left unchanged, but the controllers (CON-150 through 550 and CWS-650) were altered to match power data from the actual test. This was done for the informatics boxes (EV-701 and EV-702) as well.

To set the radiation environment for the model, a single sink temperature was iterated on until a specific Environmental Protection Garment (EPG) spot on the model matched the temperature of test data. This approach was taken because there was not a reliable estimate of the environment on any side of the xPLSS due to unreliable data from environment coupons in the TVAC test. Further, the environment likely varied from one side of the xPLSS shell

to another; this seems to be the case since the xPLSS EPG temperatures vary depending on location in the test. One way to get around this issue is to place the model within the space of a larger model accurately representing the vacuum chamber, heater cage, and various other structures impacting radiation exchange to the xPLSS. However, this would have created an unreasonable amount of work for this study and departed from the radiation setup of the original model. Thus, the comparisons made in this work will partially assess the accuracy of modeling radiation with a single sink temperature, equal in all directions.

Lastly concerning the model, it should be noted that the RCA was set to a constant half cycle time in all of the cases run. This is because tuning the coefficients governing RCA performance to match test data would have taken more time than was reasonable for this study. From a thermal perspective, as long as the motor is cycling as often as it was in the test, there is not much difference between matching the performance and simply setting a constant half cycle with no performance change. The consequence here is the caveat that this model doesn't accurately represent the vent loop fluid composition since the RCA's CO2 removal rate will not be consistent with reality.

Temperature comparisons were made at locations where valid thermocouple (TC) data was recorded during the test. The model is discretized enough in most areas to allow sampling one or more nodes to represent the location where a TC was placed on the actual xPLSS. The full list of these TCs with their lookup ID (used for reference in figures and discussion later) and a description of their actual location is provided in Table 1. As mentioned, *most* of these could be associated with nodes in the model, however the discretization level on the housings for the controllers and Spacesuit Water Membrane Evaporator (SWME) was too low to choose even one node representing their respective TCs. In those cases, the nearest node or a set of nodes around the location were sampled.

IV. Results

To validate the model over the wide range of thermal environments attempted in Chamber B testing, a single case was chosen for each of the five EVAs. These cases were chosen by looking at the transient behavior of all TCs on the xPLSS and finding any points where *most* of the temperature signals did not change by more than 1 ℉ in the leading hour. For all of the EVAs, this point was only reached near the end of the EVA due to the slow thermal response of many parts of the xPLSS as well as changes to the heater cage made over the first hour or two of an EVA.

The model inputs for the chosen cases are provided in Table 2 in the form of a case matrix. The sink temperature applied to the model is shown in the first column to the right of the EVA number, followed by the vent loop flow rate, water loop flow rate, simulated CO_2 input flow rate, metabolic H_2O input flow rate (always zero), simulated metabolic heat load, and RCA half cycle time. These values are averaged over the 60 seconds preceding the point in testing chosen for each case. The environment temperatures range from a low of -142.8 ℉ to a high of 245.5 ℉, and metabolic heat inputs range from a low of 298 BTU/hr to a high of 1973 BTU/hr. The input flow rate for simulated metabolic CO2 varies from zero input to 103.9 g/hr, which corresponds to a metabolic rate of approximately 1200 BTU/hr. Note that in the variation of RCA half cycle time, which is correlated with CO_2 input, cases 2 and 3 have very different half cycle times even though their CO_2 input flow rates are nearly identical. There was a lot of RCA performance variation in this test due to a number of issues that are still under investigation at the time of writing this paper[17]. For the purpose of this work, which is model validation, it only matters that the frequency of bed cycling matches what occurred in the test.

Table 1. List of xPLSS TC's Used for Model Comparison.

Subsystem	TC Lookup ID#	Description
Component Hardware Temperature Sensors		
xPLSS	TS-T01-050	PV-111, Primary Oxygen Vessel Front End
xPLSS	TS-T01-051	PRV-113, Primary Oxygen Regulator Linear Actuator
xPLSS	TS-T01-052	CON-150, POR Controller Housing
xPLSS	TS-T01-053	POR Regulator Monel Body
xPLSS	TS-T02-050	PV-210, Secondary Oxygen Vessel Front End
xPLSS	TS-T02-051	PRV-213, Secondary Oxygen Regulator Linear Actuator
xPLSS	TS-T02-052	CON-250, SOR Controller Housing
xPLSS	TS-T02-053	SOR Regulator Monel Body
xPLSS	TS-T03-050	GS-322, Suit Inlet Gas Sensor
xPLSS	TS-T03-051	Fan-323, Primary Fan
xPLSS	TS-T03-054	GX-380, Rapid Cycle Amine Valve Housing
xPLSS	TS-T03-055	GX-380, Rapid Cycle Amine Housing
xPLSS	TS-T04-050	CON-450, Thermal Loop Controller Housing
xPLSS	TS-T04-051	HX-440, SWME Valve Housing
xPLSS	TS-T04-052	HX-440, SWME Valve Linear Actuator
xPLSS	TS-T04-053	HX-440, Spacesuit Water Membrane Evaporator Housing
xPLSS	TS-T04-054	TCV-421 Linear Actuator
xPLSS	TS-T05-050	HX-540, Mini-Membrane Evaporator Linear Actuator
xPLSS	TS-T05-051	HX-540, Mini-Membrane Evaporator Housing
xPLSS	TS-T05-052	CON-550, Auxilliary Thermal Loop Controller Housing
xPLSS	TS-T06-051	CON-650, CWS Housing #2
xPLSS	TS-T07-051	Base of Battframe Near Backplate Contact
xINFO	TS-T07-053	INFO - EV-702 Housing Inside Face
xINFO	TS-T07-054	INFO - EV-702 Mounting Plate Bottom #1
xPLSS	TS-T01-055	Primary Regulator - Inlet from POV
xPLSS	TS-T02-055	Secondary Regulator - Inlet from SOV
xPLSS	TS-T07-056	Radio - Between Housing and Battery Rack

Table 2. xPLSS Model Simulation Case Matrix.

EVA #	Env. Temp (F)	OVL Flow Rate (acfm)	PTCL Flow Rate (lbm/hr)	CO2 Input (g/hr)	H2O Input (g/hr)	Heat Input (BTU/hr)	Half Cycle Time (s)
1	-142.8	5.6	215.0	103.9	0	586	17
2	-130.0	5.6	215.0	51.9	0	1973	297
3	245.5	5.6	215.0	51.8	0	1881	682
4	237.7	5.6	215.0	0.0	0	298	5774
5	238.0	5.6	215.0	69.1	0	363	164

Each case was run for 8 hours to achieve good thermal convergence. The final temperature values representing each TC location were taken as the average of the final 10 minutes of the 8-hour simulation, then compared to the test data from the corresponding Chamber B EVA. The absolute error in degrees Fahrenheit between simulation and TVAC is plotted against environment temperature in Figure 3 for each TC selected for comparison (note that the selection of TC's was made based on which sensors were available and providing meaningful data in all simulated EVA's). These errors are grouped into six different plots according to subsystem. With the exception of the Secondary Oxygen Assembly (SOA) and Caution and Warning System (CWS)/xINFO sets, errors are mostly positive in the cold cases and negative in the hot cases. Since the error is simulation minus actual, a positive error implies that the simulation is predicting a temperature warmer than was actually experienced. This disparity between cold and hot case errors suggests that the model is providing estimates that are actually the opposite of conservative, while conservative estimates are generally the goal of most models built for informing design (including this model). However, there are important aspects of the test that could not be captured in the model but would certainly have an effect on the temperatures under scrutiny here. Those aspects will be discussed throughout the remainder of this section. Thermal contours of the coldest case, EVA 1, and the hottest case, EVA 3, are provided in Figure 2 for more context in the coming discussion of model errors.

The Primary Oxygen Assembly (POA) and SOA temperature errors are shown in plots (a) and (b), respectively, of Figure 3. POA errors are exclusively positive in the cold cases and negative in the hot cases, while the SOA errors are generally positive in all cases and larger than the POA errors. As seen in the thermal contours of Figure 2, the SOA components are warmer than those of the POA, mainly due to heat exchange from the CWS-650 right beneath it. The main mode of exchange between the two is radiation to the Secondary Oxygen Vessel (SOV), which has a relatively large surface area. The magnitude of that exchange is similar to the radiation the SOV receives from the xPLSS cover, meaning it is one of the most significant contributors. The sum of those two contributions is then sunk into the baseplate through the frame of the SOR, a conduction pathway. Therefore, the SOA has multiple potential sources of thermal error. The low discretization of the CWS-650 may propagate error into the SOA with coarse,

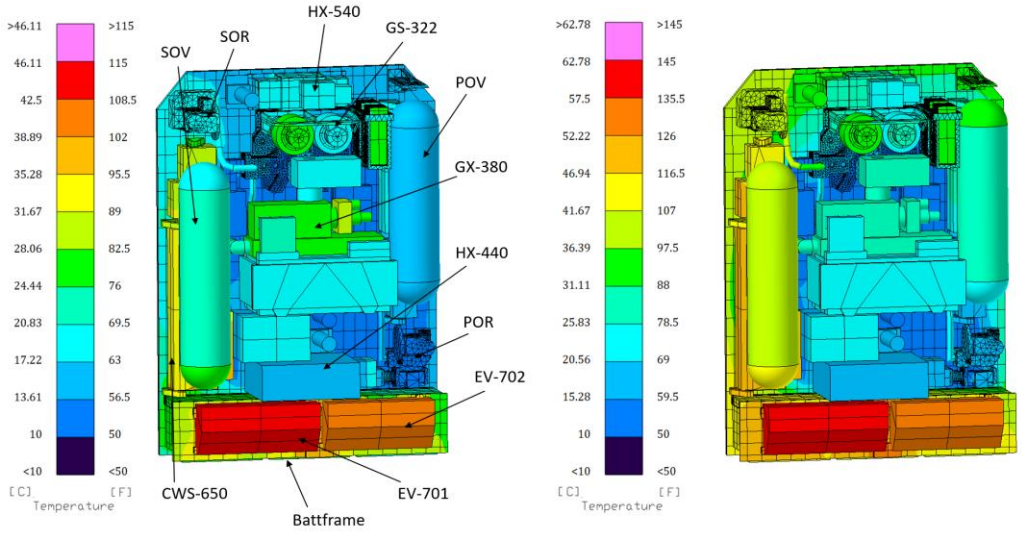

Figure 2. Thermal contours of the xPLSS TD model for the EVA 1 case (left) and EVA 3 case (right).

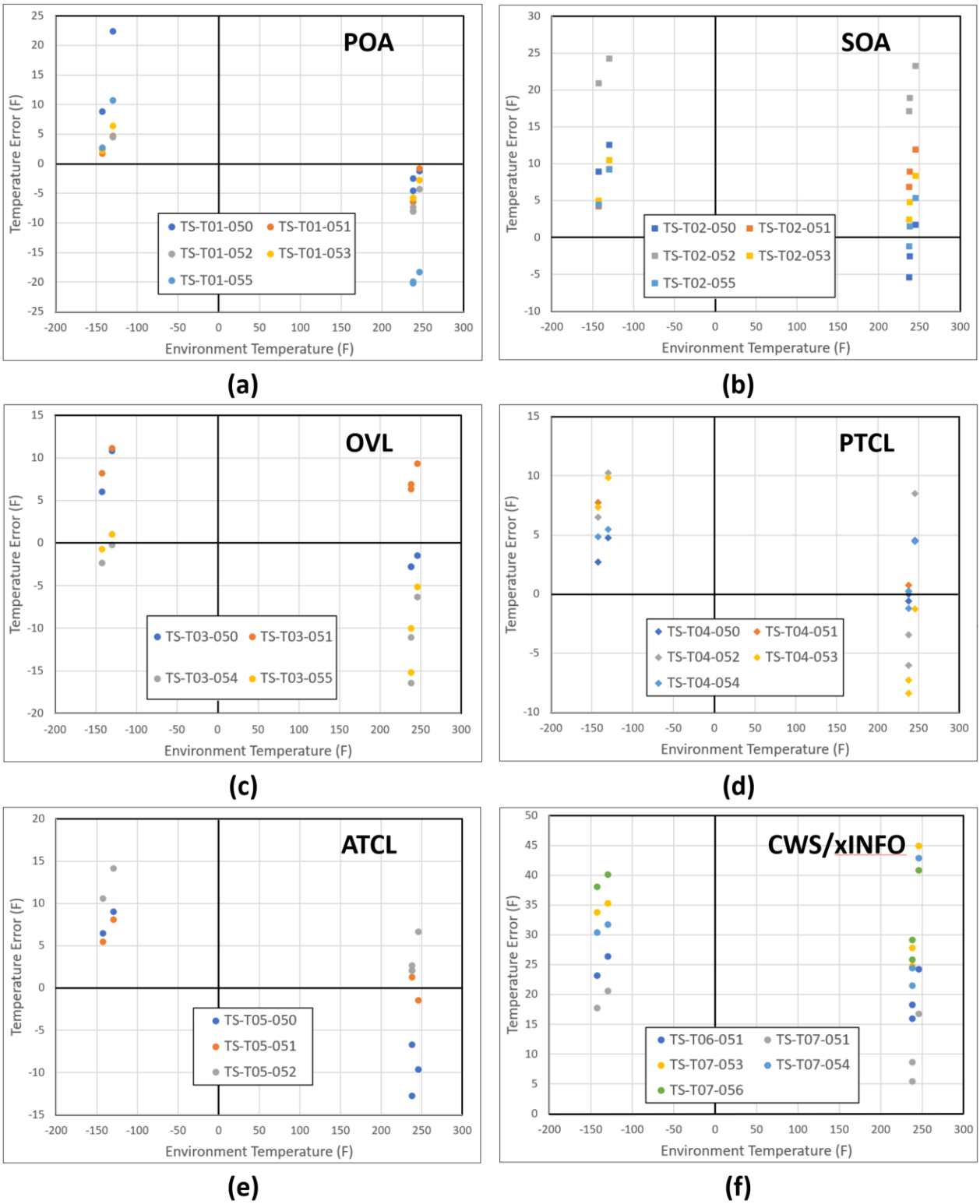

Figure 3. xPLSS model temperature errors relative to real TC data for each environment simulated. Data is grouped by subsystem: (a) POA, (b) SOA, (c) OVL, (d) PTCL, (e) ATCL, and (f) CWS/xINFO.

poorly defined gradients on its radiating faces. The SOV itself is also made up of fewer than five nodes despite its large surface area. Another considerable source of error could be the temperatures on the sides of the xPLSS cover, which are exposed to the same environment as the front side in the simulation. In the actual test, the sides were closer to ambient due to heat leak from the xPGS side of the heater cage through the mylar dividers. This would also affect the POA temperature errors; however, correcting it would further exacerbate the errors already shown by raising the temperature in the cold cases and lowering it in the hot cases. Therefore, there is more to this picture than errors from the uniformity of the environment.

The OVL temperature errors, shown in plot (c) of Figure 3, follow the same trend seen for the POA. However, the fan temperature errors, TS-T03-051, were positive in all cases and typically between 5-10 ℉. This could be due to an overestimation of the fan motor's heat dissipation, which is applied as a constant heat source in the model, or an underestimation of the strength of the conduction path sinking the fan to the baseplate. The RCA bracket errors, TS-T03-054 and -055, are large in the three hot cases with significant spread across those cases relative to the two cold ones. This is not likely due to the environment temperature because the changes from one hot case to another are not very large and because the cold cases should align with the same trend if that were the cause. In fact, plotting the absolute temperatures of the TVAC and simulation data for the RCA bracket, shown in Figure 4, reveals that while the simulation varies monotonically with environment temperature, the actual test article did not. The coldest of the three environments has a higher bracket temperature likely because of residual heat from previous steps in the metabolic profile. Before the step where that data was sampled, the motor was cycling every 15 seconds for around 45 minutes. In the other two cases, the fastest half-cycle time before the point where data was sampled was about 700 seconds. A better point in time could not be picked for the colder of the three hot environments since it was the best steady-state sample during that EVA. The other two EVAs suggest that the bracket temperatures are more sensitive to changes in environment temperature in the simulation than in TVAC. The hotter of the two environments also had a much larger metabolic heat input to the water loop that can impact the bracket temperatures. It may be that the RCA bracket in the model is overly sensitive to changes in PTCL temperatures. Running more cases while varying the inputs mentioned here may help to illuminate the cause.

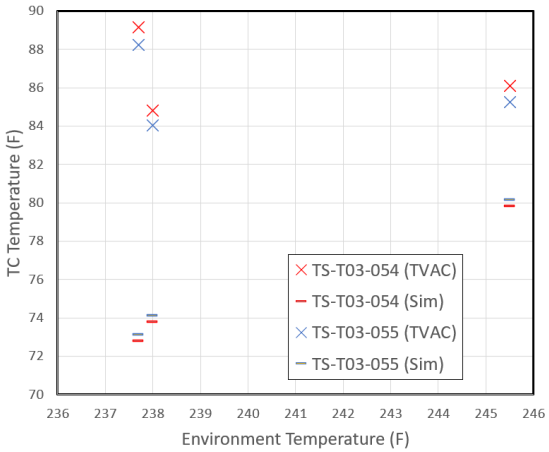

Figure 4. Comparison of absolute temperatures for RCA bracket TC locations between TVAC and Simulation.

The temperature errors on the PTCL, shown in plot (d) of Figure 3, follow the same trend seen for the POA and OVL where errors are positive in the cold cases and negative in the hot cases. The PTCL errors are generally the smallest of all the other groups analyzed, with the CON-450 housing temperatures, TS-T04-050, being the smallest of this group. The errors on the TCV linear actuator, TS-T04-054, trend similarly to the CON-450 housing errors albeit with slightly larger magnitude. There is no apparent reason why they are the smallest errors overall of any other TC comparisons, but since they are elements with specific heat loads applied, it could be that their heat loads are more accurate than the heat loads applied to other elements (e.g., CON-350, FN-323, etc.). The largest errors seen in the PTCL group are the SWME BPV motor (TS-T04-052) and housing (TS-T04-053), which are typically twice as large or more than the other errors in the PTCL group. This is most likely an issue of discretization, because the BPV and housing are each represented with a single node in the model while the other TCs are each represented by an average of four nodes on components with even more than that. The other TC comparison in this group is the BPV motor housing, TS-T04-051, but only has two viable data points since the associated TC sensor was providing erroneous data for part of the test. The two data points provide conflicting results of the model's accuracy, since one error is relatively large while the other is near zero.

Regarding the ATCL group, shown in plot (e) of Figure 3, errors trend similarly to the PTCL. The largest of these errors is on CON-550, represented by TS-T05-052. Since the CON-550 errors are all positive, it is possible that the heat dissipation applied to the component in the model was overestimated, or that its conductive path to the backplate is underestimated. The Mini-Membrane Evaporator (MiniME) motor, TS-T05-050, errors are large and of similar magnitude in both the hot and cold cases. The MiniME housing, TS-T05-051, errors are large in the cold cases but relatively smaller in the hot cases. Neither have heat loads applied to them, nor was the MiniME operating during any of the cases analyzed here. In the case of the motor, a single node represents the full component, so the

larger errors there may be due to discretization. However, the influence of the top of the xPLSS cover could be having an impact on both of these temperatures similar to the impact the sides of the xPLSS cover were earlier suggested to have on the POA and SOA components.

The temperature errors on the CWS-650, EV-701, and EV-702 are shown in plot (f) of Figure 3. As noted earlier, these are the largest errors of all groups analyzed in this study and are exclusively positive. This means the model is predicting those locations to be hotter than they were in the actual test. In the case of CWS-650, represented by TS-T06-051, discretization of the component in the model is very coarse despite its large size. It includes strong refinement at the points of contact to brackets holding it in place, however the lack of refinement on the main faces leaves errors to build up in the temperature gradients they take on. Another consequence of the CWS-650 discretization that has been alluded to already is the lack of a node(s) close to the location of the actual TC. Given the thermal gradients experienced by the component in the model, a likely source of error is difference in location between the representing node and the actual TC placed on the test article. Regarding EV-701 and EV-702, represented by the remaining TCs in this group, the most likely source of error is the heat dissipation applied to those components in the model. A value was chosen based on power data from the actual test, however the power supplied to the unit is not completely converted to heat. Further, the interior of the EV-701 and -702 are not modeled; these components are simply their thin aluminum housings with low thermal mass. Overall, it is likely the combination of inaccurate heat dissipation and low model detail that is resulting in such large errors on the EV-701 and -702 components.

V. Recommendations

The temperature errors seen for the xPLSS model as a whole are not egregious and follow a consistent trend where the cold cases predict temperatures too warm, and the hot cases predict temperatures too cold. Having discussed the trends, outliers and other nuances that came with the results of this work, the prevailing issues contributing to error seem to be component discretization, uniformity of the radiation environment, and heat dissipation applied to individual components. These changes are recommended for the xPLSS model to boost general fidelity as well as make it a better representation of the Chamber B TVAC test.

Coarse discretization and low node count were seen primarily on the housings for the SWME and MiniME and their respective BPVs. as well as the six controllers (CON-150, -250, -350, -450, -550, and CWS-650). Refining these components will improve their representation of temperature gradients and allow them to interact radiatively with other model components in a more realistic way. Modeling the thickness of the housings with an inner layer of nodes and solid elements between provides two major benefits with little additional computational cost. Firstly, it more accurately represents the thermal mass of the housing and secondly, it captures another dimension of the thermal gradient. The added cost comes in the form of just a handful of more rows in the solution matrix and, only if desired, a small radiation calculation to be made for the interior of the housing. Due to the regular shapes of every component mentioned above, a simple, structured tetrahedral mesh can be applied rather than a more complex method using TD Direct or other avenues.

The uniformity of the thermal environment is more of a case issue. It is possible to encounter a mostly uniform environment, but in the case of Chamber B TVAC the environment was much more directional and varied along the sides of the test article. Because the xPLSS model's radiation is based on a sink temperature that is applied uniformly across the whole of its exterior, it does not accurately represent the environment in the test. This can be accounted for by splitting the different sides of the xPLSS cover into individual radiation groups with their own sink temperatures. This would allow variation from side to side, but of course further divisions would be required to allow variation along a single side. This could become cumbersome for the thermal modeler, especially if there is a lot of variation along one side that they aim to capture. An alternative would be to copy the model into a model representing the vacuum chamber, heater cage, and any radiatively influential objects that appeared in the test. Then, by making this environment a radiation boundary, the xPLSS model will experience the complex directionality, reflections, etc. of the test environment. However, this could become cumbersome for the solver, especially if the environment is built with fine discretization.

Heat dissipation applied to electronic components in the xPLSS model is at best an estimate of what is applied to the actual component in test since TD is not capable of modeling the electronic generation of heat. The original model uses calculated power values from the rated voltage and current of the component, using the worst-case where applicable to be conservative. For this study, those values were replaced with power calculated from the measured voltage and current of the component. While this may be an improvement in fidelity, there is still room for uncertainty

since not all electrical energy supplied to the component is dissipated into heat. Applying an efficiency factor to the overall heat dissipation value and adjusting to match the test may yield more accurate results.

Overall, these changes will increase the general fidelity of the xPLSS model, but simple increases in detail in places that saw significant errors in this work can also go a long way. If testing of the xEMU advances to HITL at some point, having this model at a higher level of fidelity would be a great asset since it is already capable of accepting realistic metabolic inputs and could thus be used to predict performance in such a test.

Acknowledgments

The authors would like to extend their gratitude to the countless engineers and analysts who have developed the xPLSS Thermal Model over the last decade. The authors would also like to thank all of the test operators and test engineers who helped create such great thermal data. The authors would also like to thank all of the facility workers at the Chamber B facility at Johnson Space Center.

References

[1]Barnes, G, et.al., "Exploration PLSS Thermal Desktop Modeling", ICES-2019-389, *49th International Conference on Environmental Systems*, July 2019.

[2]Hutchinson, M., "Oxygen Regulator Controller (CON-150/250 Detailed Thermal Analysis [PLSS-ANAL-152], *Jacobs*,, JETS-JE33-22-TLSS-DOC-0054, September 28, 2022.

[3]Miranda, B.M.S., "Oxygen Ventilation Loop Controller/CON-350 Detailed Thermal Analysis [PLSS-ANAL-154], *Jacobs*, JETS-JE33-20-TLSS-DOC-0043, June 25, 2021.

[4]Abraham, B., "Thermal Loop Controller/CON-450 Detailed Thermal Analysis [PLSS-ANAL-155], *Jacobs*, JETS-JE33-19-TLSS-DOC-0099, September 27, 2022.

[5]Devine, M., "CON-550 Detailed Thermal Analysis [PLSS-ANAL-156]", *Jacobs*, JETS-JE33-22-TLSS-DOC-0052, September 30, 2022.

[6]Andersen, N., "EV-702 Thermal Analysis", *Jacobs*, JETS-JE33-21-TLSS-DOC-0075, July 25, 2022.

[7]Speasmaker, L., "Actuator and TCV-420 Detailed Thermal Analysis", *Jacobs*, JETS-JE33-19-TAED-DOC-0025, May 28, 2020.

[8]Andersen, N., "Common Actuator Linear Potentiometer Accuracy [PLSS-ANAL-196], *Jacobs*, JETS-JE33-21-TLSS-DOC-0005, August 3, 2021.

[9]Lipke, S., "Multi-Gas Sensor (GS-322/GS-300) Detailed Thermal Analysis for xEMU [PLSS-ANAL-186], *Jacobs*, JETS-JE33-19-TLSS-DOC-0125, August 4, 2022.

[10]Lipke, S., "PD-691 Battery Interface Circuit Detailed Thermal Analysis and IVA Dissipation for In-Situ Charge [PLSS-ANAL-168]. *Jacobs*, JETS-JE33-20-TLSS-DOC-0009, November 21, 2022.

[11]Thornton, C., "Antenna (ANT-764A/ANT-764B) Detailed Thermal Analysis [PLSS-ANAL-208]", *Jacobs*, JETS-JE33-20-TLSS-DOC-0015, September 14, 2022.

[12]Lancaster, B., "Evaluate Microgravity Impacts on PLSS Primary Oxygen Vessel (POV)/PV-111, Secondary Oxygen Vessel (SOV)/PV-210 Inside/Outside Temperature Correlation, and Caution & Warning System (CWS) Consumable Calculations", *Jacobs*, JETS-JE33-21-TLSS-DOC-0081, September 7, 2022.

[13]Thornton, C., "EVA Consumables Assessment for xEMU [PLSS-ANAL-183]", *Jacobs*, JETS-JE33-20-TLSS-DOC-0055, September 12, 2022.

[14]Barnes, B., "EVA Abort Analysis of OSS Modified LCVG", *Jacobs*, JETS-JE33-14-TAED-DOC-0139, October 21, 2014.

[15]Andersen, N. "Primary Thermal Control Loop Faults with Excessive Cooling Assessment [PLSS-ANAL-243]", *Jacobs*, JETS-JE33-21-TLSS-DOC-0020, August 10, 2022.

[16]Barrett, L & B.M.S. Miranda, "Thermal Control Valve (TCV-421) Auto-Cooling Control Update for Environment/Variable Avionics Load [PLSS-ANAL-207]", *Jacobs*, JETS-JE33-20-TLSS-DOC-0068, May 18, 2021.

[17]Westheimer, D., Rodriggs, L., Falconi, E., Swartout, B., and Lewandowksi, C., "xEMU Thermal Vacuum Testing Overview," International Conference on Environmental Systems, ICES, Louisville, KY, 2024.